Dye-Sensitized Photocatalytic Hydrogen Production Promoted by Near-Infrared Pyrrolopyrrole Cyanine Sensitizers

Thibaut Baron, Deborah Romito, Léo Corne, Baptiste Andrin, Yann Pellegrin, Fabrice Odobel

Dye-sensitized Photocatalytic Hydrogen Production Promoted by Near-Infrared Pyrrolopyrrole Cyanines Sensitizers

Thibaut Baron,[a] Deborah Romito,[a] Léo Corne,[a] Baptiste Andrin,[a] Yann Pellegrin,[a] and Fabrice Odobel[a]*

[a]Nantes Université, CNRS, CEISAM, UMR 6230, F-44000 Nantes, France. E-mail: Fabrice.Odobel@univ-nantes.fr

Supporting Information Placeholder

ABSTRACT: The indispensable need for clean and sustainable energy sources has recently favored a deeper interest in dye-sensitized photocatalytic systems (DSPs) for hydrogen production. In this work, a pyrrolopyrrole cyanine (**TB207**) near-infrared (NIR) photosensitizer (PS) is grafted over surface-platinized TiO_2 nanoparticles (NPs) for photocatalytic H_2 evolution. Preliminary experiments deal with determining the optimal dye and Pt^0 loadings, as well as opportunely choosing the pH of the aqueous reaction medium. The resulting photocatalytic system exhibits about 400 turnover numbers (TON_{PS}) in presence of ascorbic acid (AA) at pH 4 after 6 hours of irradiation with a sunlight simulator (1000 W/m^2). At last, co-sensitization of **TB207** with Eosin Y (**EY**), a complementary visible light absorber, is tested both in dye-sensitized solar cells (DSSCs) and DSPs, demonstrating an enhancement of the solar energy conversion performances of the cocktail dyes in both devices over the single absorber systems, due to better light harvesting.

KEYWORDS: near infrared dyes, solar fuel, dye-sensitized photocatalysis, hydrogen evolution, dye sensitized solar cell, Eosin Y, co-sensitization.

Introduction

The urgent need for the transition from fossil fuels to renewable and environmentally friendly energy sources has spurred a growing interest in solar driven dihydrogen (H_2) production,[1] having this molecule the highest energy content per weight. Furthermore, its combustion exclusively releases water, a non-toxic and benign compound.[2] The utilization of H_2 finds large applications, being required for ammonia synthesis and chemical industry, refining, synthetic fuels and power generation.[3] However, more than 95% of current H_2 production is far from being carbon-neutral, since it still derives from the steam reforming or the partial oxidation of fossil sources.[4] This has recently promoted a strong interest towards the H_2 generation by using sunlight as energy source,[5] with the best performances achieved by using photovoltaic cells coupled to electrolysers, resulting in photon-to-H_2 conversion yields up to 30%.[6, 7] Nevertheless, this technology requires expensive and highly complex working set-ups, which strongly limits their further development in large scale. Aiming at a simpler and cheaper photocatalytic system, a significant effort has been invested in sensitizing colloidal nanoparticles (NPs) of metal oxide semiconductors (SCs) with organic molecular chromophores or transition metal complexes, resulting in Dye-Sensitized Photocatalytic systems (DSPs).[8, 9] Notably, what makes this technology highly appealing for photocatalytic H_2 production is its simplicity of preparation, potential low cost and facility to scale-up. Indeed, the system simply consists of n-type SC NPs (titanium oxide TiO_2 being the most used) coated with a photosensitizer (PS) and a Hydrogen Evolution Catalyst (HEC). Upon irradiation, the photosensitizer absorbs a photon and passes into its excited state (PS*), which can inject an electron in the conduction band (CB) of TiO_2. At last, H_2 evolution is achieved when the resulting electron diffuses to the HEC, while the photo-oxidized photosensitizer PS^+ is regenerated by a sacrificial electron donor (SED) in solution. Hence, an ideal photocatalytic system must possess good light harvesting properties (namely : intense and broad absorption features spanning over the visible spectrum), as well as thermodynamically favorable Gibbs free enthalpies for electron injection (ΔG°_{inj}) and PS^+ regeneration (ΔG°_{reg}),[10, 11] which explains how crucial is the choice of the PS. Among the dyes employed for the photocatalytic H_2 production, the vast majority of chromophores essentially absorbs sunlight in the visible range (Figure 1). Notably, tris-bipyridine Ru(II) complexes have been extensively investigated as PSs.[12] However, aiming at overcoming their low extinction molar coefficient and their potential high cost due to the presence of expensive and rare metal, fully organic chromophores have been successfully implemented into DSPs, such as phenothiazine,[13] xanthene,[14] coumarin[15] or carbazole-based[16] sensitizers, yielding respectable efficiencies.[17, 18]

In sharp contrast, only handful examples exploiting PSs absorbing in the near-infrared (NIR) region have been reported for the photocatalytic H_2 production in DSP systems, in spite of the fact that exploiting NIR photons would enhance the overall solar energy to hydrogen conversion effiency.[17-23] The main reason is that the implementation of NIR absorbers implies a low energy lying excited state (due to the red-shifted absorption), making injection and/or regeneration of the PS challenging steps. In 2019, one study dealt with a BODIPY-based core, covalently bound to a phenothiazine to achieve a main absorption band at 638 nm, which produced up to 70 µmol·mg^{-1} of H_2.[21] Squaraine dyes display absorption maxima up to 680 nm, such as that reported by *Kim* and co-workers, having a strong absorption centered at 684 nm.[24] When grafted over TiO_2 NPs encapsulated in graphene oxide, the resulting system led to the H_2 production of about 40 µmol in one hour. At last, zinc phthalocyanines have been employed as NIR dyes (having their absorption maxima extended up to 699 nm) in DSPs with significant performances.[20, 25, 26] As far as we are aware, there are no example describing NIR dyes with maxima of absorption beyond 750 nm, which are investigated for photocatalytic hydrogen production through DSPs.

We recently reported the utilization of **TB207**, a symmetrical pyrrolopyrrole cyanine (*PPcy*), for the development of fully transparent and colorless Dye Sensitized Solar Cells (DSSCs) with

remarkable success,[27] and this prompted us to investigate its suitability for H_2 production in DSP systems (Figure 1). Following the classical procedure for DSPs, where the organic dye is grafted on TiO_2-Pt^0 NPs, we optimized experimental parameters, such as dye and Pt-loading concentrations, pH of the aqueous solution and also the irradiation sources, resulting in a recorded TON_{PS} over 400 for H_2 production. Moreover, photo-amperometry measurements were carried out in order to afford more details about the efficiencies of our systems.

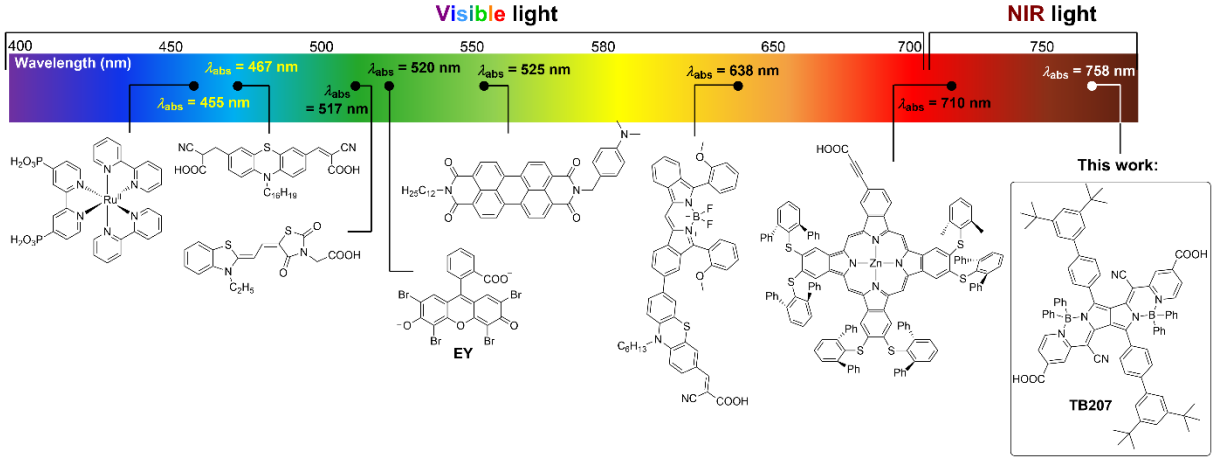

Figure 1. Selected examples of classically dyes used in DSPs in different wavelength windows, including **EY** and **TB207**, employed in this work.

Finally, we performed co-sensitization of **TB207** with Eosin Y (**EY**) to build panchromatic DSSC and DSP devices with broad absorption over the visible-NIR range. Hence, our study globally shines light on the capability of low-photon energy absorbing dyes (750 nm) for photocatalytic proton reduction, paving the way for future more efficient devices exploiting a broader range of sunlight wavelengths.

Results and Discussion

The photophysical and electrochemical properties of **TB207** are summarized in Table 1 and its absorption and emission spectra are shown in Figures 2, S1-S2. The dye exhibits the peculiar absorption features of pyrrolopyrrole cyanine compounds, displaying a sharp π-π* transition at 758 nm and a weaker vibronic band at 685 nm. The dye also possesses an intense emission band at 772 nm, with a lifetime τ_{em} of 3.2 ns and a fluorescence quantum yield of 0.6 in ethanol (Figure S3). At pH 4, the electron injection driving force in the CB of TiO_2 is weak (-0.16 eV), but still significant to be guaranteed, while the regeneration reaction is thermodynamically allowed only for ascorbic acid (AA) as SED ($\Delta G°_{reg}$ = -0.35 eV), suggesting that **TB207** could satisfyingly meet the energetic requirements to work in DSP with AA as SED.

The photocatalytic system consists in nanoparticles of TiO_2 coated first with Pt^0 as HEC and then with **TB207** as PS (see ESI for detailed description). To validate the grafting of **TB207** onto TiO_2 through the carboxylic acid moieties, infrared (IR) spectroscopy measurements were performed on powdery **TB207** and on the functionalized **TB207**/TiO_2/Pt^0 NPs (Figure S4). This results in a variation of the ν(C=O) stretching of the free carboxylic acid units

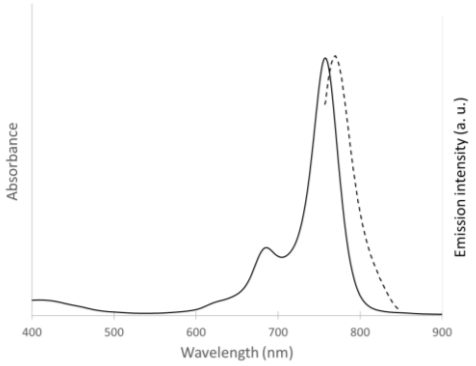

Figure 2. Normalized absorption (straight line) and emission (dashed line) spectra of **TB207** recorded in CH_2Cl_2 solution.

in **TB207**, marked by an intense and sharp band at 1715 cm^{-1}, which is no longer observed in the IR spectrum of **TB207**/TiO_2/Pt^0 NPs (Figure S1). In addition, there is the appearance of the asymmetric and symmetric stretching bands of O-C=O between 1600-1650 cm^{-1} and at 1382 cm^{-1} respectively, accounting for the chelation of carboxylic acid to TiO_2 surface.

In order to choose the most suitable SED for this photocatalytic system, a preliminary photoelectrochemical study was performed. Towards this objective, photosensitizer **TB207** was chemisorbed on nanocrystalline TiO_2 films screen-printed on FTO-covered glass (see ESI for detailed preparation). The resulting electrodes were tested by performing chopped light Linear Sweep Voltammetry (LSV) at a steady potential of 0 V *vs.* SCE in aqueous solutions of triethanolamine (TEOA) or AA as SEDs at different pH (Figure 3). The current density recorded using TEOA is extremely weak with a value reaching 3.1 at pH 6 (Figure 3a). This is consistent with the TEOA oxidation potential of +0.85 V *vs.* SCE, eventually resulting in a zero $\Delta G°_{reg}$ which makes the dye regeneration thermodynamically very unfavorable (Table 1). In sharp contrast, employing AA as SED drastically improves the photocurrent density, notably achieving a 100-fold increase of the recorded photocurrent density

(about 250 µA/cm^2 at pH 4 – red line in Figure 3b) due to the much more favorable Gibbs free Enthalpy of electron injection (-0.35 eV). However, the generated photocurrent is halved by increasing the pH of one unit (black line in Figure 3b), and keeps on decreasing down to 50 µA/cm^2 at pH 8 (green line). The negative impact of alkaline conditions with AA is not related to the regeneration reaction efficiency, but to the increase of the energy level of the TiO_2 conduction band (CB), limiting the electron injection driving force. This limitation is the direct consequence of the usually low reducing power of NIR dyes (for example the $\Delta G°_{inj}$ of **TB207** drops to +0.1 eV at pH = 8, while it is -0.16 eV at pH = 4).

Photocatalytic measurements

The H_2 evolution photocatalytic experiments were conducted on 10 mg of **TB207**/TiO_2/Pt^0 NPs suspended in 5 mL of an aqueous solution containing either TEOA or AA, irradiated with different light sources (see below and experimental part) and the H_2 production was monitored by analyzing the composition of the headspace atmosphere by gas chromatography (GC). In agreement with the photoelectrochemical investigations, upon irradiation of **TB207**/TiO_2/Pt^0 functionalized NPs in the presence of TEOA as SED, no H_2 production could be observed.

Table 1. Photophysical and electrochemical properties of **TB207**, all potentials are referenced *vs.* saturated calomel electrode (SCE). Calculated Gibbs free energies for electron injection (ΔG_{inj}) and dye regeneration (ΔG_{reg}).

$\lambda_{abs}/\varepsilon$ (nm/M^{-1}·cm^{-1})	λ_{em} (nm)	τ_{em} (ns)	ϕ_{em}	E_{00}[a] (eV)	E^b (S^+/S) (V)	E^a (S/S^-) (V)	E^c (S^+/S^*) (V)	[c]ΔG_{inj} (eV)	[d]ΔG_{reg} AA (eV)	[d]ΔG_{reg} TEOA (eV)
685/35900; 758/138000	772	3.2	0.60	1.60	0.80	-0.80	-0.80	-0.16	-0.35	0

[a] calculated with E_{00} = 1240 eV/λ_{inter}, with λ_{inter} = wavelength (in nm) at the intersection of the normalized absorption and emission spectra; [b]determined in V *vs.* SCE; [c]calculated at pH = 4 according to $\Delta G_{inj} = E(S^+/S) - E_{00} + E_{CB}(TiO_2)$ with $E_{CB}(TiO_2) = -0.4 - 0.059 \cdot pH$;[28] [d]calculated according to $\Delta G_{reg} = E(SED^+/SED) - E(S^+/S)$, with SED = Sacrificial Electron Donor and $E(AA^+/AA)$ = 0.47 V *vs.* SCE, and $E(TEOA^+/TEOA)$ = 0.85 V *vs.* SCE.

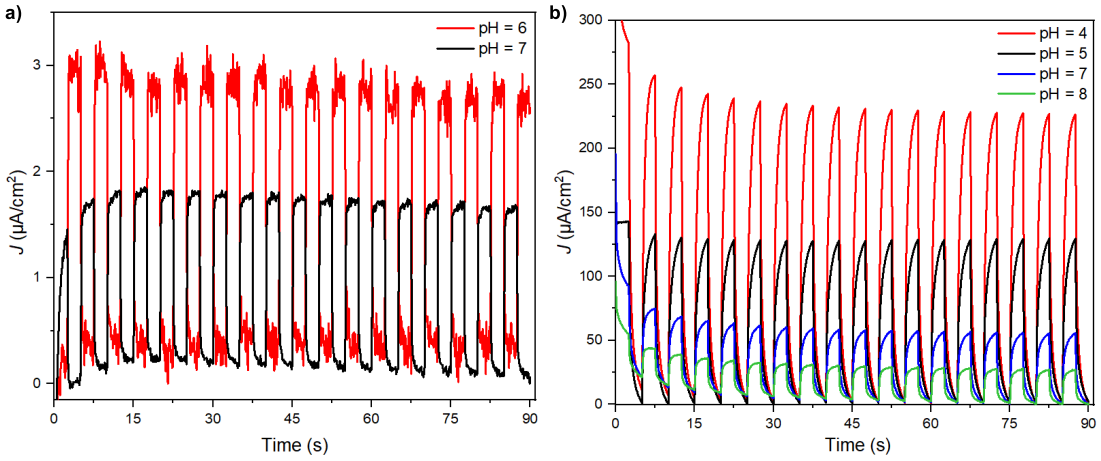

Figure 3. Chopped-light chronoamperometric measurements recorded under red light with LED irradiation (λ_{excit} = 737 nm, power 238 W/m^2) of **TB207** on a TiO_2 film in the presence of *a)* TEOA (15% v/v) and *b)* 0.1 M AA at different pHs. All experiments were recorded as a function of time with an applied potential of 0 V *vs.* SCE.

Contrarily, replacing TEOA with AA as SED in the DSP system promoted H_2 evolution, thanks to the effective regeneration of the PS^+ (Table 2).

The photocatalytic performances were further optimized by screening the pH of the aqueous reaction medium. In analogy with the LSV experiments, the highest amounts of H_2 were obtained at pH 4 (7.23 µmol, TON_{PS} = 391), whereas lower quantities were produced at pH 3 and 5 (4.81 and 3.46 µmol, respectively). The efficiency of H_2 evolution drops at pH 3 *versus* pH 4 (Table 2, Figures 4 and S5) can be explained by the change of the oxidation potential of ascorbic acid according to the pH (pKa(AA) =3.95).[29] Below the pKa, the major species in solution if the fully protonated ascorbic acid; whose oxidation potential is 0.93 V *vs.* SCE, while above pKa AA is mono-deprotonated and the anionic species displays a less positive oxidation potential (0.47 V *vs.* SCE), which makes the regeneration reaction thermodynamically more favorable. Knowing the tendency of **TB207** to aggregate, that usually negatively affects the electron injection quantum yield by self-quenching,[27] we have investigated the impact of adding variable concentrations of chenodeoxycholic acid (CDCA) to the **TB207** dyeing bath.[30, 31] Nevertheless, the resulting photocatalytic H_2 production decreases upon increased amounts of CDCA, being more than halved after three hours of irradiation when a ratio of 1/50 for **TB207**/CDCA is tested, while only 0.36 µmol of H_2 are measured with **TB207**/CDCA in ratio 1/100 (Figure S7). Adding CDCA to

the dyeing bath does not significantly hinder the **TB207** chemisorption over TiO_2 NPs, as displayed by the almost identical amounts of **TB207** found on TiO_2 without CDCA or in the presence of 5 mM of CDCA (**TB207** loading: 6.39 and 6.84 nmol/TiO_2 mg, respectively). The cause behind this experimental result remains obscure, but it is consistent with another study showing that CDCA does not necessarily improve the photocatalytic performances of an organic dye in DSPs.[30]

The third screened parameter was the dye loading of **TB207** onto the functionalized TiO_2 NPs. Towards this objective, surface-platinized TiO_2 NPs were soaked in **TB207** solutions having different concentrations (0.1, 0.05 and 0.025 mM, respectively). The optimum H_2 production was measured with a dye loading corresponding to 4.7 nmol/TiO_2 mg, since almost 10 µmol of H_2 could be produced after irradiating the DSP system for 5 hours. Furthermore, the resulting TON_{PS} is almost twice the value achieved with a higher dye loading (417 for 4.7 *vs* 261 for 6.4 nmol/TiO_2 mg, respectively), proving that a compromise must be achieved between an efficient light harvesting (proportional to the dye loading) and the dye aggregation.

Finally, the optimal Pt^0 loading was determined by screening different surface-platinized TiO_2 NPs, using a dye loading of 4.7 nmol/TiO_2 NPs in the presence of 0.1 M AA aqueous solution at pH 4 (Figure S8). As predictable, the lowest amount of $0.39 \cdot 10^{-7}$ mol/TiO_2 mg of Pt^0 produces less H_2 (1.22 µmol corresponding to a TON_{PS} of 52). Surprisingly, no significant difference in the H_2 production could be observed using $0.67 \cdot 10^{-7}$ mol/TiO_2 mg of Pt^0, and almost doubling its concentration to $1.23 \cdot 10^{-7}$ mol/TiO_2 mg (3.04 *vs* 2.53 µmol, respectively). This highlights how crucial it is to find a balance between a high Pt^0 loading (which directly promotes the electron injection from the PS*) and a lower one (decreasing the occurrence of parasitic charge recombination reactions). Indeed, a recent study from Mallouk and co-workers[32] revealed a very subtle correlation between the Pt nanoparticle size on the electron injection and charge recombination kinetic. High Pt^0 loading results in a larger size for the Pt particles and promotes the electron injection from the PS excited state, but also accelerates charge recombination reaction. Conversely, a lower Pt^0 loading slows down charge recombination reaction, which is important to maximize the dye regeneration efficiency with the sacrificial electron donor. To conclude the screening, the H_2 generation is tripled up to 9.71 µmol by using a Pt^0 loading of $2.92 \cdot 10^{-7}$ mol/TiO_2 mg, leading to a TON_{PS} of 413, while the highest Pt^0 loading of $5.43 \cdot 10^{-7}$ mol/TiO_2 mg only promotes H_2 production of about 4 µmol. Control experiments indicate that there is no detectable H_2 production without light irradiation, in absence of sacrificial electron donor, or by irradiation with 740 nm LED of bare TiO_2 nanoparticles (Pt° but without chemisorbed dye). This proves that H_2 is generated according to a photochemical process upon photoexcitation of **TB207** and its regeneration by the SED. In addition, the apparent quantum yield (AQY) at 740 nm is 1.3% as calculated with the real LED flux that reaches the reactional mixture (ESI for details).

Table 2. Photocatalytic results of our DSP systems recorded under different conditions[a].

Entry	Dye(nmol)/TiO_2(mg)/Pt^0(10^{-7}mol)	pH	SED	Light source	H_2	
					µmol	TON_{PS}
1	**TB207**(3.7)/TiO_2/Pt^0(3.2)	3	AA	Two LEDs 740 nm	4.81 ± 0.14	259 ± 8
2	**TB207**(3.7)/TiO_2/Pt^0(3.2)	4	AA	Two LEDs 740 nm	7.23 ± 0.4	391 ± 22
3	**TB207**(3.7)/TiO_2/Pt^0(3.2)	5	AA	Two LEDs 740 nm	4.12 ± 0.3	222 ± 16
4	**TB207**(3.7)/TiO_2/Pt^0(3.2)	8	TEOA	Two LEDs 740 nm	N.D.[b]	-
5	**TB207**(3.7)/CDCA(1:50)/TiO_2/Pt^0(3.2)	4	AA	Two LEDs 740 nm	3.4	134
6	**TB207**(3.7)/CDCA(1:100)/TiO_2/Pt^0(3.2)	4	AA	Two LEDs 740 nm	0.36	17
7	**TB207**(2.1)/TiO_2/Pt^0(3.2)	4	AA	Two LEDs 740 nm	1.97	187
8	**TB207**(4.7)/TiO_2/Pt^0(3.2)	4	AA	Two LEDs 740 nm	9.79 ± 1.3	417 ± 55
9	**TB207**(6.4)/TiO_2/Pt^0(3.2)	4	AA	Two LEDs 740 nm	8.35 ± 1.2	261 ± 37
10	**TB207**(4.7)/TiO_2/Pt^0(0.39)	4	AA	Two LEDs 740 nm	1.22	51
11	**TB207**(4.7)/TiO_2/Pt^0(0.67)	4	AA	Two LEDs 740 nm	3.04	129
12	**TB207**(4.7)/TiO_2/Pt^0(1.23)	4	AA	Two LEDs 740 nm	2.53	107
13	**TB207**(4.7)/TiO_2/Pt^0(1.49)	4	AA	Two LEDs 740 nm	4.09	174
14	**TB207**(4.7)/TiO_2/Pt^0(2.92)	4	AA	Two LEDs 740 nm	9.71± 1.3	413± 55

15	**TB207**(4.7)/TiO_2/Pt^0(2.92)	4	AA	Sun Simulator	9.09± 1.2	387± 51
16	**TB207**(4.7)/TiO_2/Pt^0(2.92)	4	AA	Natural Sunlight	7.71	328

[a]The following standard conditions were employed: 5 mL of 0.1 M SED in water (at pH 4 for AA, pH 8 for TEOA) + 10 mg of functionalized TiO_2 NPs; irradiation time: 6 hours. [b]Not detected: N.D.

To investigate the ability of **TB207** to work under the solar spectrum, additional photocatalytic measurements were performed by irradiation with a sunlight simulator AM 1.5 [1000 W/m^2] and under external natural solar light (Figure 4 and Table 2). The resulting H_2 evolution decreases between 1 and 2 µmol, respectively, when both artificial and natural sunlights are used compared with the red LED irradiation (2 LEDs at 740 nm, 5.45 mW each), since a turnover number (TON) of 387 and 328, respectively, were determined, while the corresponding experiment with the LED lights leads to a TON_{PS} of 417. This supports the hypothesis that **TB207** could work in natural sunlight conditions and with even higher performances than with the narrow range wavelength of LED sources. Moreover, the lower quantity of H_2 evolved under natural *versus* artificial sunlight can be explained by the variable incidence angle of the sun during the experiment (6 hours). This, inevitably, changes the insulating power on the sample due to the Earth rotation, while the intensity of the sun simulator stays constant throughout the whole experiment. Inspection of the H_2 production as a function of time (Figure S6), indicates that it declines after 5-6 hours of irradiation. To shed some light on the origin of the performances decrease, **TB207** was desorbed from the NPs after 6 hours of photocatalysis under simulated sunlight and the absorption spectrum of the buffer solution was also recorded (Figure S9). On one hand, after photocatalysis, there remains only 33% of non-degraded dye on TiO_2 nanoparticles. On the other hand, the absorption spectrum of the buffer solution does not display significant absorbance around 740 nm. This proves that the main cause of the performance's loss comes the dye bleaching.

Cocktail dyes towards panchromatic light induced H_2 production

The above results prove that a NIR photosensitizer such as **TB207** can be effectively used to produce H_2 using low energy photons in the far red of the solar spectrum. A widely used strategy in DSSCs to expand the light harvesting efficiency (LHE) consists in co-absorbing several PSs on the TiO_2 surface.[33, 34] There are rare examples of implementation of this approach in DSP, although it could in principle enhance the photocatalytic H_2 production.[19, 35, 36] Here, a xanthene dye, Eosin Y (**EY**) was chosen as visible light harvester owing to its complementary absorption spectrum with **TB207** (Figures S10-S11). In spite of the many successful examples of cocktail dyes in DSSCs, there are also many combinations of dyes which failed to provide higher photovoltaic efficiency due to the enhancement of charge recombination promoted by one dye, resulting in overall poorer performances.[37] Accordingly, we firstly studied the photovoltaic performances of **TB207** and **EY** (Table 3). The absorption spectra on TiO_2 show that **EY** must be in large excess in order to be sufficiently chemisorbed on the TiO_2 surface, probably because of its lower tendency to absorb onto TiO_2 due to its hindered anchoring group, which limits the approach of the dye to TiO_2 surface (Figure S10). Looking at the photovoltaic performances of the cocktail dyes, it can be observed that the mixture of **TB207** and **EY** in a 1/3 ratio provides significantly higher photovoltaic performances than the single dye (Table 3). This can be understood as the consequence of favorable higher LHE (Figure S10) as confirmed by the broader Incident Photon-to-electron Conversion Efficiency (IPCE) (Figure 5). Clearly, **TB207** collects and transforms photons into electricity between 600 and 800 nm, while **EY** is active in the region between 400 and 550 nm, further highlighting the effectiveness of using these two dyes for a broader light collection.

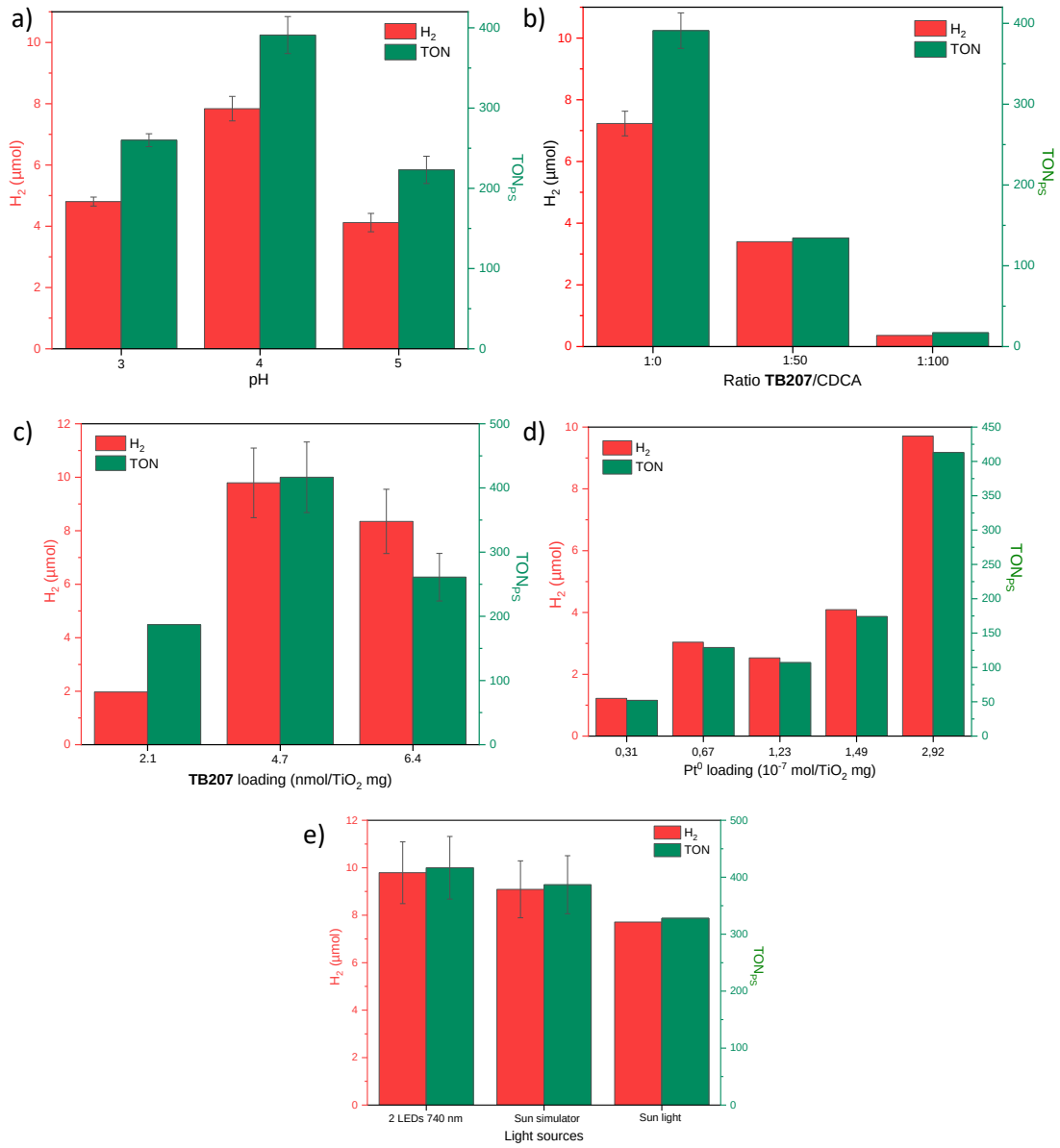

Figure 4. Photocatalytic H_2 production measured with **TB207**/TiO_2/Pt^0 functionalized NPs in DSP systems, with the corresponding µmol of H_2 generated and the TON_{PS} as a function of *a)* the pH of the 0.1 M AA aqueous solution used as reaction medium, *b)* the amount of CDCA co-absorbed with **TB207** on the TiO_2 NPs, at pH = 4, *c)* the dye loading at pH = 4, *d)* the Pt^0 loading at pH = 4 and *e)* the different light sources used to irradiate the system in the optimum conditions.

Table 3. Photovoltaic performances of DSSCs fabricated with different **TB207/EY** ratios, recorded under simulated sunlight AM 1.5 (100 mW/cm^2).

TB207/EY ratio	J_{SC} (mA/cm^2)	V_{OC} (mV)	FF (%)	PCE (%)
1/0	2.96 ± 0.1	406 ± 5	47 ± 1	0.58 ± 0.06
3/1	5.19	418	61	1.33
1/1	6.14	432	59	1.57

1/3	6.69	423	59	1.66
1/5	1.53	421	52	0.33
1/10	1.92	437	53	0.44
0/1	3.36	432	62	0.90

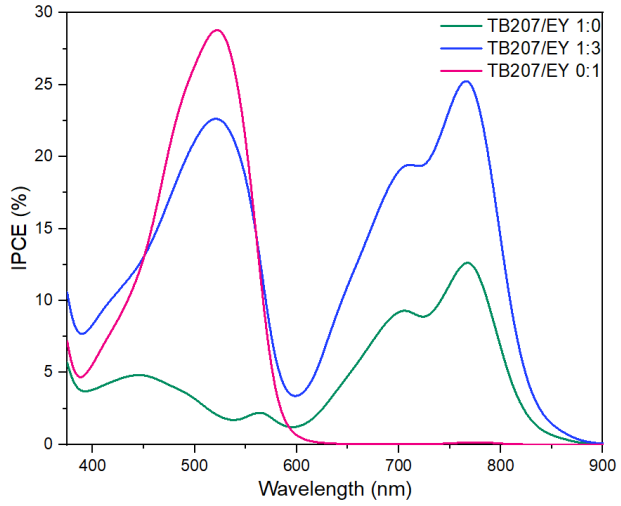

Figure 5. IPCE spectra of DSSCs co-sensitized with **TB207** (green line), **EY** (pink line) and both dyes in ratio 1/3 (blue line).

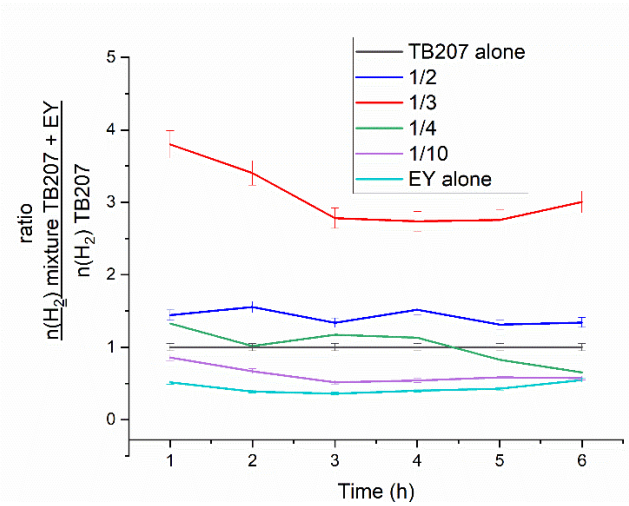

Figure 6. Photocatalytic H_2 production achieved by DSPs based on TiO_2/Pt^0 NPs functionalized with **TB207** and **EY** recorded under sunlight simulator (30 mW/cm^2).

The successful combination of **TB207** with **EY** in DSSC prompted us to investigate the H_2 evolution activity of this cocktail in DSP systems having TiO_2 NPs functionalized with different amounts of the dyes, with a 0.1 M AA aqueous solution at pH 4 as reaction medium, and the sunlight simulator as irradiation source (Figures 6 and S10). At first, it appears that in these conditions, **EY** alone produces less H_2 than **TB207**. Secondly, in agreement with the photovoltaic results in DSSCs, the mixture of dyes **TB207**/**EY** with the ratios 1/2 and 1/3 enable better H_2 photogeneration when compared to the dyes **TB207** and **EY** alone, by a factor of more than 3 fold. Overall, these results demonstrate the advantage of using multiple PSs to improve the light harvesting in DSP and thus the overall solar fuel efficiency as it was shown in DSSC. Accordingly, the development of NIR absorbers for DSP will certainly be valuable to improve solar to fuel conversion efficiency when they are associated with an efficient dye absorbing in the visible range, as they are many in the literature.

Conclusion

This study demonstrates the photocatalytic H_2 production in DSPs based, for the first time, on apyrrolopyrrole cyanine dye **TB207**, standing for the most red-shifted NIR photosensitizer used for this application. Optimizing the experimental conditions by modulating the pH of the aqueous reaction media and by screening dye and Pt^0 loading allows to achieve a TON of about 400 within 6 hours of irradiation, demonstrating the effective H_2 production with low energy photons such as 1.60 eV in DSPs. Moreover, this dye is effective even under natural sunlight irradiation, thus proving its practical interest. Finally, successful co-sensitization of **TB207** with a complementary visible light eosin based dye (**EY**) both in DSSCs and DSP systems, provides a concrete example that solar energy to chemical energy conversion efficiency of these systems can be boosted.Previous studies[27, 38] of **TB207** on TiO_2 by transient absorption spectroscopy and by intensity-modulated photovoltage/photocurrent spectroscopy (IMVS/PS) experiments showed that the performances are mainly controlled by the electron injection quantum yield, which is limited by the weak driving force and the formation of aggregates. Taking into account the large number of possible functionalization of pyrrolopyrrole cyanine dyes, introduction of bulky and electron rich substituents on this type of dye should overcome these limitations.

We expect that this study will contribute to develop better performing DSPs in the future by the design of new NIR absorbing PSs and their implementation with visible light PSs.

ASSOCIATED CONTENT

Supporting Information

The Supporting Information is available free of charge on the ACS Publications website at DOI:

Experimental details, photocatalytic H_2 evolution results, FTIR spectra and additional data (PDF)

AUTHOR INFORMATION

Corresponding Authors

*Fabrice.Odobel@univ-nantes.fr

Notes

The authors declare no competing financial interests.

ACKNOWLEDGMENT

We acknowledge financial support by Agence National de la Recherche (ANR) through the program Vision-NIR (ANR-17-CE05-0037-02) and for the project Solar-H2 financed by EUR LUMOMAT (Investments for the Future program ANR-18-EURE-0012). We warmly thank Simon Ali Rincon Celis and Stefan Haacke (IPCMS, UMR 7504, 67034 Strasbourg, France) for the measurement of the fluorescence quantum yield of **TB207**.

REFERENCES

(1) Shafiei, E.; Davidsdottir, B.; Leaver, J.; Stefansson, H.; Asgeirsson, E. I. Energy, economic, and mitigation cost implications of transition toward a carbon-neutral transport sector: A simulation-based comparison between hydrogen and electricity. *J. Cleaner Prod.* **2017**, *141*, 237-247.
(2) Uyar, T. S.; Beşikci, D. Integration of hydrogen energy systems into renewable energy systems for better design of 100% renewable energy communities. *Int. J. Hydrogen Energy* **2017**, *42* (4), 2453-2456.
(3) Cherkasov, N.; Ibhadon, A.; Fitzpatrick, P. A review of the existing and alternative methods for greener nitrogen fixation. *Chemical Engineering and Processing* **2015**, *90*, 24-33.
(4) Rodriguez, J. Production d'hydrogène par photocatalyse et conversion électrochimique dans une pile à combustible. Université de Grenoble, PhD Thesis,, 2013.
(5) Rzayeva, M.; Salamov, O.; Kerimov, M. Modeling to get hydrogen and oxygen by solar water electrolysis. *Int. J. Hydrogen Energy* **2001**, *26* (3), 195-201.
(6) Khaselev, O.; Bansal, A.; Turner, J. High-efficiency integrated multijunction photovoltaic/electrolysis systems for hydrogen production. *Int. J. Hydrogen Energy* **2001**, *26* (2), 127-132.
(7) Jia, J.; Seitz, L. C.; Benck, J. D.; Huo, Y.; Chen, Y.; Ng, J. W. D.; Bilir, T.; Harris, J. S.; Jaramillo, T. F. Solar water splitting by photovoltaic-electrolysis with a solar-to-hydrogen efficiency over 30%. *Nat. Commun.* **2016**, *7* (1), 13237.
(8) Willkomm, J.; Orchard, K. L.; Reynal, A.; Pastor, E.; Durrant, J. R.; Reisner, E. Dye-sensitised semiconductors modified with molecular catalysts for light-driven H 2 production. *Chem. Soc. Rev.* **2016**, *45* (1), 9-23.
(9) Warnan, J.; Willkomm, J.; Ng, J. N.; Godin, R.; Prantl, S.; Durrant, J. R.; Reisner, E. Solar H 2 evolution in water with modified diketopyrrolopyrrole dyes immobilised on molecular Co and Ni catalyst–TiO 2 hybrids. *Chem. Sci.* **2017**, *8* (4), 3070-3079.
(10) Grätzel, M. Recent advances in sensitized mesoscopic solar cells. *Acc. Chem. Res.* **2009**, *42* (11), 1788-1798.
(11) Anderson, A. Y.; Barnes, P. R.; Durrant, J. R.; O'Regan, B. C. Quantifying regeneration in dye-sensitized solar cells. *J. Phys. Chem. C* **2011**, *115* (5), 2439-2447.
(12) Bae, E.; Choi, W.; Park, J.; Shin, H. S.; Kim, S. B.; Lee, J. S. Effects of surface anchoring groups (carboxylate vs phosphonate) in ruthenium-complex-sensitized TiO2 on visible light reactivity in aqueous suspensions. *J. Phys. Chem. B* **2004**, *108* (37), 14093-14101.
(13) Lee, J.; Kwak, J.; Ko, K. C.; Park, J. H.; Ko, J. H.; Park, N.; Kim, E.; Ahn, T. K.; Lee, J. Y.; Son, S. U. Phenothiazine-based organic dyes with two anchoring groups on TiO 2 for highly efficient visible light-induced water splitting. *Chem. Commun.* **2012**, *48* (93), 11431-11433.
(14) Kurimoto, K.; Yamazaki, T.; Suzuri, Y.; Nabetani, Y.; Onuki, S.; Takagi, S.; Shimada, T.; Tachibana, H.; Inoue, H. Hydrogen evolution coupled with the photochemical oxygenation of cyclohexene with water sensitized by tin (IV) porphyrins by visible light. *Photochem. Photobiol. Sci.* **2014**, *13* (2), 154-156.
(15) Abe, R.; Sayama, K.; Arakawa, H. Significant influence of solvent on hydrogen production from aqueous I3−/I− redox solution using dye-sensitized Pt/TiO2 photocatalyst under visible light irradiation. *Chem. Phys. Lett.* **2003**, *379* (3-4), 230-235.
(16) Lai, H.; Liu, X.; Zeng, F.; Peng, G.; Li, J.; Yi, Z. Multicarbazole-based D− π–A dyes sensitized hydrogen evolution under visible light irradiation. *ACS Omega* **2020**, *5* (4), 2027-2033.
(17) Reginato, G.; Zani, L.; Calamante, M.; Mordini, A.; Dessì, A. Dye-Sensitized Heterogeneous Photocatalysts for Green Redox Reactions. *Eur. J. Inorg. Chem.* **2020**, *2020* (11-12), 899-917.
(18) Huang, J. F.; Lei, Y.; Luo, T.; Liu, J. M. Photocatalytic H2 Production from Water by Metal-free Dye-sensitized TiO2 Semiconductors: The Role and Development Process of Organic Sensitizers. *ChemSusChem* **2020**, *13* (22), 5863-5895.
(19) Sun, Y.; Sun, Y.; Dall'Agnese, C.; Wang, X.-F.; Chen, G.; Kitao, O.; Tamiaki, H.; Sakai, K.; Ikeuchi, T.; Sasaki, S.-i. Dyad sensitizer of chlorophyll with indoline dye for panchromatic photocatalytic hydrogen evolution. *ACS Appl. Energy Mater.* **2018**, *1* (6), 2813-2820.
(20) Tiwari, A.; Krishna, N. V.; Giribabu, L.; Pal, U. Hierarchical porous TiO2 embedded unsymmetrical zinc–phthalocyanine sensitizer for visible-light-induced photocatalytic H2 production. *J. Phys. Chem. C* **2018**, *122* (1), 495-502.
(21) Suryani, O.; Higashino, Y.; Sato, H.; Kubo, Y. Visible-to-near-infrared light-driven photocatalytic hydrogen production using dibenzo-BODIPY and phenothiazine conjugate as organic photosensitizer. *ACS Appl. Energy Mater.* **2018**, *2* (1), 448-458.
(22) Ding, H.; Xu, M.; Zhang, S.; Yu, F.; Kong, K.; Shen, Z.; Hua, J. Organic blue-colored DA-π-A dye-sensitized TiO2 for efficient and stable photocatalytic hydrogen evolution under visible/near-infrared-light irradiation. *Renewable Energy* **2020**, *155*, 1051-1059.
(23) Kotani, H.; Miyazaki, T.; Aoki, E.; Sakai, H.; Hasobe, T.; Kojima, T. Efficient near-infrared light-driven hydrogen evolution catalyzed by a saddle-distorted porphyrin as a photocatalyst. *ACS Appl. Energy Mater.* **2020**, *3* (4), 3193-3197.
(24) Joseph, K. V.; Lim, J.; Anthonysamy, A.; Kim, H.-i.; Choi, W.; Kim, J. K. Squaraine-sensitized composite of a reduced graphene oxide/TiO 2 photocatalyst: π–π stacking as a new method of dye anchoring. *J. Mater. Chem. A* **2015**, *3* (1), 232-239.
(25) Genc Acar, E. l.; Yuzer, A. C.; Kurtay, G.; Yanalak, G.; Harputlu, E.; Aslan, E.; Ocakoglu, K.; Gullu, M.; Ince, M.; Patir, I. H. Improving the Photocatalytic Hydrogen Generation Using Nonaggregated Zinc Phthalocyanines. *ACS Appl. Energy Mater.* **2021**, *4* (9), 10222-10233.
(26) Yıldız, B.; Güzel, E.; Akyüz, D.; Arslan, B. S.; Koca, A.; Şener, M. K. Unsymmetrically pyrazole-3-carboxylic acid substituted phthalocyanine-based photoanodes for use in water splitting photoelectrochemical and dye-sensitized solar cells. *Sol. Energy* **2019**, *191*, 654-662.

(27) Baron, T.; Naim, W.; Nikolinakos, I.; Andrin, B.; Pellegrin, Y.; Jacquemin, D.; Haacke, S.; Sauvage, F.; Odobel, F. Transparent and Colorless Dye-Sensitized Solar Cells Based on Pyrrolopyrrole Cyanine Sensitizers. *Angew. Chem. Int. Ed.* **2022**, *134* (35), e202207459.
(28) Kavan, L.; Tétreault, N.; Moehl, T.; Grätzel, M. Electrochemical characterization of TiO2 blocking layers for dye-sensitized solar cells. *J. Phys. Chem. C* **2014**, *118* (30), 16408-16418.
(29) Macartney, D. H.; Sutin, N. The oxidation of ascorbic acid by tris(2,2′-bipyridine) complexes of osmium(III), ruthenium(III) and nickel(III) in aqueous media: Applications of the Marcus cross-relation. *Inorg. Chim. Acta* **1983**, *74*, 221-228.
(30) Manfredi, N.; Monai, M.; Montini, T.; Peri, F.; De Angelis, F.; Fornasiero, P.; Abbotto, A. Dye-sensitized photocatalytic hydrogen generation: efficiency enhancement by organic photosensitizer–coadsorbent intermolecular interaction. *ACS Energy Lett.* **2017**, *3* (1), 85-91.
(31) Zhang, X.; Yu, L.; Zhuang, C.; Peng, T.; Li, R.; Li, X. Highly asymmetric phthalocyanine as a sensitizer of graphitic carbon nitride for extremely efficient photocatalytic H2 production under near-infrared light. *ACS Catal.* **2014**, *4* (1), 162-170.
(32) Nishioka, S.; Hojo, K.; Saito, D.; Yamamoto, I.; Mallouk, T. E.; Maeda, K. The effects of Pt cocatalyst particle size on charge transfer kinetics in dye-sensitized SrTiO3 photocatalysts for hydrogen evolution studied by time-resolved emission/absorption spectroscopy. *Appl. Catal., A* **2023**, *654*, 119086.
(33) Yum, J.-H.; Baranoff, E.; Wenger, S.; Nazeeruddin, M. K.; Grätzel, M. Panchromatic engineering for dye-sensitized solar cells. *Energy Environ. Sci.* **2011**, *4* (3), 842-857.
(34) Cole, J. M.; Pepe, G.; Al Bahri, O. K.; Cooper, C. B. Cosensitization in dye-sensitized solar cells. *Chem. Rev.* **2019**, *119* (12), 7279-7327.
(35) Ho, P. Y.; Mark, M. F.; Wang, Y.; Yiu, S. C.; Yu, W. H.; Ho, C. L.; McCamant, D. W.; Eisenberg, R.; Huang, S. Panchromatic Sensitization with ZnII Porphyrin-Based Photosensitizers for Light-Driven Hydrogen Production. *ChemSusChem* **2018**, *11* (15), 2517-2528.
(36) Nikolaou, V.; Charalambidis, G.; Landrou, G.; Nikoloudakis, E.; Planchat, A.; Tsalameni, R.; Junghans, K.; Kahnt, A.; Odobel, F.; Coutsolelos, A. G. Antenna Effect in BODIPY-(Zn) Porphyrin Entities Promotes H2 Evolution in Dye-Sensitized Photocatalytic Systems. *ACS Appl. Energy Mater.* **2021**, *4* (9), 10042-10049.
(37) Otaka, H.; Kira, M.; Yano, K.; Ito, S.; Mitekura, H.; Kawata, T.; Matsui, F. Multi-colored dye-sensitized solar cells. *J. Photochem. Photobiol., A* **2004**, *164* (1-3), 67-73.
(38) Kurucz, M.; Nikolinakos, I.; Soueiti, J.; Baron, T.; Grifoni, F.; Naim, W.; Pellegrin, Y.; Sauvage, F.; Odobel, F.; Haacke, S. Transparent Near-IR Dye-Sensitized Solar Cells: Ultrafast Spectroscopy Reveals the Effects of Driving Force and Dye Aggregation. *ChemPhotoChem* **2024**, e202300175. DOI: 10.1002/cptc.202300175.

Graphical abstract for entry
Dye-sensitized Photocatalytic Hydrogen Production Promoted by Near-Infrared Pyrrolopyrrole Cyanines Sensitizers

Thibaut Baron,[a] Deborah Romito,[a] Léo Corne,[a] Baptiste Andrin,[a] Yann Pellegrin,[a] and Fabrice Odobel[a]*

[a]Nantes Université, CNRS, CEISAM, UMR 6230, F-44000 Nantes, France. E-mail: Fabrice.Odobel@univ-nantes.fr